Determinants of Anion Permeation in the Second Transmembrane Domain of the Mouse Bestrophin-2 Chloride Channel

Zhiqiang Qu and Criss Hartzell

Department of Cell Biology and the Center for Neurodegenerative Disease, Emory University School of Medicine, Atlanta, GA 30322

ABSTRACT Bestrophins have been proposed to constitute a new family of Cl channels that are activated by cytosolic Ca. We showed previously that mutation of serine-79 to cysteine in mouse bestrophin-2 (mBest2) altered the relative permeability and conductance to SCN. In this paper, we have overexpressed various mutant constructs of mBest2 in HEK-293 cells to explore the contributions to anion selectivity of serine-79 and other amino acids (V78, F80, G83, F84, V86, and T87) located in the putative second transmembrane domain (TMD2). Residues selected for mutagenesis were distributed throughout TMD2, but mutations at all positions changed the selectivity. The effects on selectivity were rather modest. Replacement of residues 78, 79, 80, 83, 84, 86, or 87 with cysteine had similar effects: the permeability of the channel to SCN relative to Cl (P_{SCN}/P_{Cl}) was decreased three- to fourfold and the relative SCN conductance (G_{SCN}/G_{Cl}) was increased five- to tenfold. Side chains at positions 78 and 80 appeared to be situated close to the permeant anion, because the electrostatic charge at these positions affected permeation in specific ways. The effects of charged sulfhydryl-reactive MTS reagents were the opposite in the V78C and F80C mutants and the effects were partially mimicked by substitution of F80 with charged amino acids. In S79T, switching from Cl to SCN caused slow changes in G_{SCN}/G_{Cl} ($\tau = 16.6$ s), suggesting that SCN binding to the channel altered channel gating as well as conductance. The data in this paper and other data support a model in which TMD2 plays an important role in forming the bestrophin pore. We suggest that the major determinant in anion permeation involves partitioning of the permeant anion into an aqueous pore whose structural features are rather flexible. Furthermore, anion permeation and gating may be linked.

KEY WORDS: chloride channels • ion permeation • electrophysiology • mutagenesis • ion channel

INTRODUCTION

Bestrophins have been proposed to constitute a new family of Cl channels that are activated by cytosolic Ca (Sun et al., 2002; Qu and Hartzell, 2003; Tsunenari et al., 2003; Qu et al., 2004; Pusch, 2004). The suggestion that bestrophins are Cl channels is supported by several lines of evidence. (a) Mutations in human best-1 produce an early-onset macular degeneration known as Best vitelliform macular dystrophy (Petrukhin et al., 1998). This disease is characterized by decreased amplitude of the slow light peak component of the electro-retinogram, suggesting that an ion channel defect may be responsible for the pathology (Francois et al., 1967; Deutman, 1969). Because the slow light peak of the electro-retinogram has been linked to a basolateral Cl conductance in retinal pigment epithelial cells (Gallemore et al., 1998), it has been suspected for some time that hBest1 is a Cl channel. hBest1 may play a role in ion transport in the retina and in regulating the ionic environment around photoreceptor cells. hBest1 has been shown to be localized in or near the basolateral membrane of retinal pigment epithelial cells (Marmorstein et al., 2000). (b) Vertebrates have four genes that code for bestrophins and *C. elegans* has >25 bestrophin genes. All bestrophins that have been tested from various species from human to worms induce Ca-activated Cl currents when overexpressed in several cell lines (Sun et al., 2002; Hartzell and Qu, 2003; Qu and Hartzell, 2003; Qu et al., 2004). The currents differ somewhat in their rectification and kinetic properties depending on the subtype of bestrophin expressed (Sun et al., 2002; Hartzell and Qu, 2003; Tsunenari et al., 2003). The dependence of the current on the type of bestrophin provides a dose of confidence that the Cl currents are not artifacts of heterologous expression. (c) Overexpressed bestrophin appears at the cell surface as assessed by cell-surface biotinylation or immunocytochemical criteria (Hartzell and Qu, 2003; Qu et al., 2004). (d) Substitution of certain amino acids in hBest1 and mBest2 with cysteine results in Cl currents that can be modified with sulfhydryl-reactive MTS reagents (Tsunenari et al., 2003; Qu et al., 2004). (e) Mutation of serine-79 to cysteine results in Cl currents with altered

Address correspondence to Criss Hartzell, Department of Cell Biology, Emory University School of Medicine, 615 Michael St., Whitehead Building 535, Atlanta, GA 30322-3030. Fax: (404) 727-6256; email: criss.hartzell@emory.edu

Abbreviations used in this paper: CFTR, cystic fibrosis transmembrane conductance regulator; mBest2, mouse bestrophin-2; TMD, transmembrane domain.

J. Gen. Physiol. © The Rockefeller University Press • 0022-1295/2004/10/371/12 $8.00
Volume 124 October 2004 371–382
http://www.jgp.org/cgi/doi/10.1085/jgp.200409108

permeability and conductance, particularly to SCN (Qu et al., 2004). Because ion permeability and conduction are controlled by the partitioning of the ion into the channel pore and the binding of the ion to sites in the permeation pathway, the mutational data provide prima facie evidence that bestrophins contribute to the pore of the Cl channel (Pusch, 2004).

Because serine-79, which we mutated in our previous paper, is located in the putative second transmembrane domain (TMD2), in this paper we have investigated the role of other residues in TMD2 in anion permeability in mBest2. The question that we sought to address was whether S79 was a key residue in determining the biophysical properties of the channel or whether other residues contributed to anion selectivity. To date, structure–function relationships have been studied extensively only in three families of cloned Cl channels: the ligand-gated anion channels like the $GABA_A$ and glycine receptors (Keramidas et al., 2002b), the cystic fibrosis transmembrane conductance regulator CFTR (Dawson et al., 1999), and the ClC channel family (Fahlke, 2001). Ligand-gated anion channels select among permeant ions based mainly on charge. Mutations in one or a few key amino acids can convert the channel from anion to cation selective. In contrast, CFTR and the ClC channels have selectivity filters composed of clusters of a number of amino acids located in more than one TMD (Dawson et al., 1999; Linsdell et al., 2000; Dutzler et al., 2002). In these channels, changes in selectivity can be introduced by mutations in an abundance of amino acid residues, but the changes in selectivity are seldom as dramatic as one observes in K channels where mutations can cause >100-fold changes in relative permeability (Armstrong, 2003). The modest changes (<10-fold) in selectivity in CFTR and ClC channels are probably related to the fact that these channels have low intrinsic selectivity and that permeation does not depend as precisely on the details of the pore as it does in K channels.

Here we show that mutations in seven different amino acids in mBest2 produce changes in anion permeability and conduction consistent with a model of the bestrophin channel pore in which the details of the structure of the pore are not as important in determining selectivity as the lyotrophic nature of the permeant anions and their partitioning into an aqueous pore.

MATERIALS AND METHODS

Site-specific Mutations of mBest2 and Heterologous Expression

Site-specific mutations of mouse bestrophin-2 (mBest2) were made using a PCR-based site-directed mutagenesis kit (Quickchange; Stratagene) as described previously (Qu et al., 2004). mBest2 cDNA (ATCC, IMAGE clone ID: 4989959, GENBANK/EMBL/DDBJ accession no. BC031186 and NM_145388) and its mutants in pCMV-SPORT6 vector were cotransfected into HEK293 cells (ATCC) using Fugene-6 transfection reagent (Roche). pEGFP (Invitrogen) was also transfected at a 10:1 ratio to identify transfected cells. To obtain modest amplitude of Ca^{2+}-activated Cl^- currents (1–2 nA per cell), 0.05 ~ 0.1 μg mBest2 wild type or 0.025 ~ 0.3 μg mBest2 mutant DNA was used to transfect one 35-mm culture dish. 1 d after transfection, cells were dissociated and replated on glass coverslips for electrophysiological recording. Transfected cells were identified by EGFP fluorescence and used for patch clamp experiments within 3 d after transfection.

With the F80R and F80E mutants, the behavior of the currents seemed to depend on the level of expression. When the usual amounts of cDNA were used for transfection, ~50% of EGFP-expressing cells had very small currents when cotransfected with the F80E mBest2, whereas ~50% of the cells cotransfected with F80R had huge currents that were not well voltage clamped. When the amount of cDNA was adjusted to give moderately sized currents, this heterogeneity disappeared.

Electrophysiology

Recordings were performed using the whole-cell recording configuration of the patch clamp technique. Patch pipettes were made of borosilicate glass (Sutter Instrument Co.), pulled by a Sutter P-2000 puller (Sutter Instrument Co.), and fire polished. Patch pipettes had resistances of 2–3.5 MΩ filled with the standard intracellular solution (see below). The bath was grounded via a 3 M KCl agar bridge connected to a Ag/AgCl reference electrode. Solution changes were performed by perfusing the 1-ml chamber at a speed of ~4 ml/min. Experiments were performed with 100 or 200-ms duration voltage ramps from −100 to +100 mV. The start-to-start interval was 2 or 10 s. Data were acquired by an Axopatch 200A amplifier controlled by Clampex 8.1 via a Digidata 1322A data acquisition system (Axon Instruments). Experiments were conducted at room temperature (20–24°C). Liquid junction potentials were measured using the liquid junction potential calculator in Clampex 8.1 to correct E_{rev} of various bionic conditions. Rectification ratios (RR) were determined from the quotient of the slope conductance measured at +50 mV from the reversal potential divided by the slope conductance measured at −50 mV from the reversal potential.

The standard pipette solution contained (in mM) 146 CsCl, 2 $MgCl_2$, 5 (Ca^{2+})-EGTA, 8 HEPES, 10 sucrose, pH 7.3, adjusted with NMDG. The free [Ca^{2+}] in the solution was determined as described by Tsien and Pozzan (1989) (Kuruma and Hartzell, 2000). The calculated Ca^{2+} concentration in the "high Ca intracellular solution" was confirmed as 4.5 μM by fura-2 (Molecular Probes) measurements using an LS-50B luminescence spectrophotometer (Perkin Elmer). The standard extracellular solution contained (in mM) 140 NaCl, 5 KCl, 2 $CaCl_2$, 1 $MgCl_2$, 15 glucose,10 HEPES, pH 7.3 with NaOH. This combination of solutions set E_{rev} for Cl^- currents to zero, while cation currents carried by Na or Cs would have very positive or negative E_{rev}, respectively. When Cl^- was substituted with another anion, NaCl was replaced on an equimolar basis with NaX, where X is the substitute anion. Solution osmolarity was 303 mOsm for both intra- and extracellular solutions (Micro Osmometer, Model 3300; Advanced Instrument). Small differences in osmolarity were adjusted by addition of glucose. DIDS (Molecular Probes) was suspended in water at 50 mM as a stock before working solutions were made.

Sulfhydryl Modification

MTSET (2-trimethylammonioethylmethanethiosulfonate, bromide), MTSES (sodium [2-sulfonatoethyl] methanethiosulfonate) (Toronto Research Chemicals), and NEM (*N*-ethylmaleimide) (Pierce Chemical Co.) were prepared in water, stored on ice, and used within 90 min. The standard extracellular solution

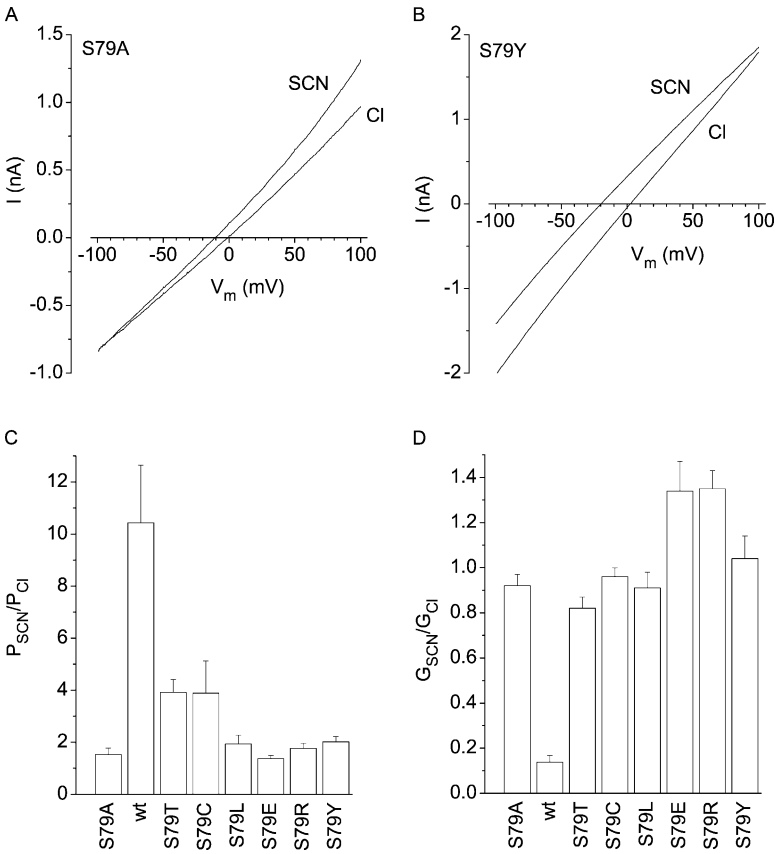

FIGURE 1. Effects of various mutations at position 79 of mBest2 on the relative permeability and relative conductance of SCN. Serine-79 in mBest2 was mutated into alanine (A), threonine (T), cysteine (C), leucine (L), glutamate (E), arginine (R), or tyrosine (Y) by site-directed mutagenesis. The mutants were separately cotransfected into HEK293 cells with EGFP vectors to mark transfected cells. Single green cells were selected for whole-cell voltage clamp recordings with a high intracellular free [Ca]. The membrane potential was held at 0 mV, stepped to −100 mV for 200 ms, and ramped from −100 mV to 100 mV in 200 ms. Start-to-start interval time was 10 s. Bath solution was either standard solution or one in which 140 mM Cl was replaced with SCN. (A and B) Effect of external SCN on the steady-state current–voltage relationships in S79A (A) and S79Y (B) mutants. I–V relationships obtained after switching to SCN were plotted for representative cells. (C) Average relative permeability ratios (P_{SCN}/P_{Cl}) of S79 mutants. The relative permeability was calculated from the Goldman-Hodgkin-Katz equation using the difference in reversal potentials with Cl or SCN in the bath. (D) Average relative conductance ratios (G_{SCN}/G_{Cl}) of SCN and Cl in S79 mutants. Ratios of conductance with SCN or Cl in the bath were obtained from the measurement of the slope of the current–voltage relationship between −25 and +25 mV from reversal potentials. The bars show the means ± SEM with cell number of 8 (S79A), 6 (S79C), 7 (wild type), 10 (S79T), 3 (S79L), 10 (S79Y), 4 (S79R), and 3 (S79E). The reversal potentials and slope conductances were obtained from the first trace after SCN application.

with the reagents diluted to the indicated working concentration was made immediately before use.

Analysis of Data

For the calculations and graphical presentation, we used OriginPro 7.0 software (Microcal). Data are expressed as mean ± SEM. Relative permeability of the channels was determined by measuring the shift in E_{rev} upon changing the bath solution from one containing 151 mM Cl^- to another with 140 mM X and 11 mM Cl^-, where X is the substitute anion (Qu and Hartzell, 2000). The permeability ratio was estimated using the Goldman-Hodgkin-Katz equation: $P_x/P_{Cl} = [Cl^-]_i/([X]_o \exp(\Delta E_{rev}F/RT)) - [Cl^-]_o/[X]_o$, where ΔE_{rev} is the difference between the reversal potential with the test anion X and that observed with symmetrical Cl^-, and F, R, and T have their normal thermodynamic meanings.

RESULTS

Channel Selectivity Is Altered Similarly by Different Amino Acid Side Chains at Position 79

We have previously shown that partial replacement of extracellular Cl with SCN blocks Cl conductance in cells expressing wild-type mBest2 (Qu et al., 2004). The SCN block was virtually abolished by mutation of serine-79 to cysteine. These data suggested that S79 was located near the anion binding site of the channel. To explore further the role of S79 in anion binding, we mutated S79 to other amino acids and determined the effects of these mutations on Cl and SCN conductances. Each of these substitutions produced measurable currents. I–V curves for representative mutations S79A and S79Y are shown in Fig. 1 (A and B), and the mean relative permeabilities and conductances for all the mutations are shown in Fig. 1 (C and D). With each of the mutations, the relative SCN permeability was less than for wild type (Fig. 1 C), and the SCN conductance was similar to or greater than the Cl conductance (Fig. 1 D), suggesting that SCN binding was reduced in these mutants in the same way as we have described for S79C. The fact that most of the amino acid substitutions that were made disrupted channel function in qualitatively similar ways suggests that serine in position 79 plays an important role in the pore. However, because none of these mutations alter the selectivity sequence for anions (Table I; unpublished data), channel permeability does not appear to be strongly dependent on the amino acid side chains at this position.

Kinetics of SCN Conductance Block

The behavior of the Thr substitution at position 79 differed from the behavior of other mutations. Although G_{SCN}/G_{Cl} was near 1 immediately after changing to SCN,

TABLE I

Anion Selectivity and Conductance of Wild-type, S79C, F80C, and F80R mBest2 Currents

	P_X/P_{Cl}				G_X/G_{Cl}			
	SCN	NO_3	I	Br	SCN	NO_3	I	Br
Wild type	13.2 ± 3.5	2.1 ± 0.2	2.0 ± 0.2	1.5 ± 0.1	0.2 ± 0.1	4.1 ± 0.7	1.7 ± 0.5	0.8 ± 0.1
S79C	3.9 ± 0.1[b]	2.5 ± 0.3	1.9 ± 0.1	1.4 ± 0.03	1.0 ± 0.1[b]	1.6 ± 0.1[b]	1.4 ± 0.1	1.0 ± 0.02
F80C	2.7 ± 0.3[a]	1.8 ± 0.1	1.7 ± 0.03	1.4 ± 0.1	1.2 ± 0.1[b]	2.0 ± 0.2[a]	1.5 ± 0.1	1.1 ± 0.03
F80R	3.3 ± 0.3[a]	2.9 ± 0.2	2.2 ± 0.1	1.5 ± 0.04	1.0 ± 0.2[b]	1.4 ± 0.1[b]	1.0 ± 0.1	1.0 ± 0.1[a]

P_X/P_{Cl} and G_X/G_{Cl} were determined as in Fig. 1.

[a]$P < 0.05$.

[b]$P < 0.01$, between wild type and mutations calculated from two-tailed *t* test. Wild type ($n = 5$), S79C ($n = 6$), F80R ($n = 4$–6), and F80C ($n = 5$).

with time, the conductance decreased so that at steady state the conductance was similar to wild type. To examine the kinetics of block, the voltage clamp protocol was changed to deliver 100-ms duration voltage ramps every 2 s (Fig. 2). Fig. 2 A compares the I–V curves obtained 4 s and 66 s after shifting to SCN-containing solution. Within 4 s after starting addition of SCN to S79T-expressing cells, the I–V relationship was shifted to the left as expected from the higher SCN permeability, but the slope conductance was not significantly changed in the same time period (Fig. 2 A). Within 66 s after changing the solution, the conductance had decreased significantly. In Fig. 2 B, the E_{rev} and the slope conductance (G_{slope}) are plotted with time after switching to SCN-containing solution for S79T-expressing cells. E_{rev} changed to a new steady value within 4 s after starting to change the bath solution (Fig. 2 B, open circles). This time reflects the time required to completely exchange the bathing solution. The slope conductance, however, changed much more slowly (Fig. 2 B, solid squares). About a minute was required for the conductance to decline to a new steady value. The decrease in conductance was fitted to a single exponential with a time constant of 16.6 s (Fig. 2 C). This suggests that SCN may affect channel gating and that the S79T mutation slows either SCN binding or the conformational change induced by SCN binding.

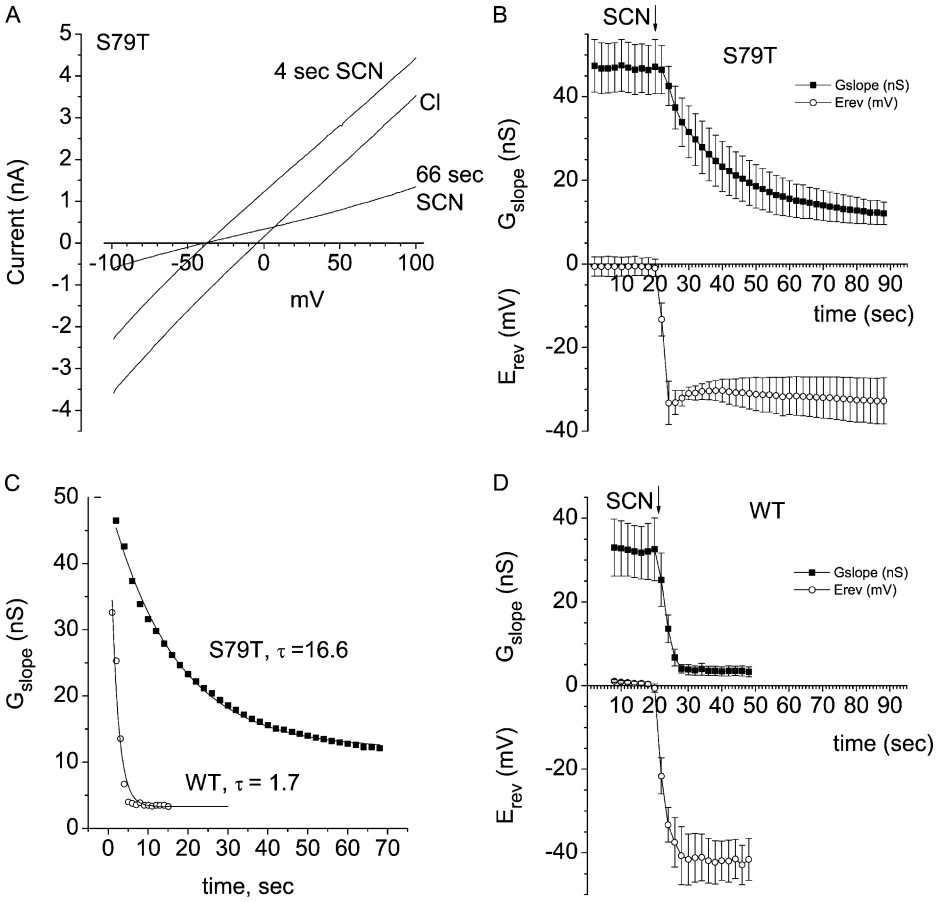

FIGURE 2. SCN slowly blocks conductance in mBest2 S79T mutants. Experiments were performed as indicated in Fig. 1 except a 100-ms duration voltage ramp was applied every 2 s. (A) Current–voltage relationships in Cl bath solution and 4 s and 66 s after switching to SCN bath solution. Note that 4 s after changing to SCN solution, the conductance of S79T did not change, but E_{rev} had shifted. After 66 s in SCN, the conductance had decreased to a minimum. (B and D) Time course of the changes in conductance and reversal potentials in S79T (B, $n = 5$) and wild type (WT) (D, $n = 5$) after switching the bath to SCN solution. G_{slope} was measured as indicated in Fig. 1. (C) Time constants for SCN effect. G_{slope} after SCN application in B and D was plotted as a function of time. The curves are the best fits to a single exponential. The apparent time constant (τ) is 16.6 s for S79T but 1.7 s for wild type (WT). The time constant for wild type reflects the time required to change the bath.

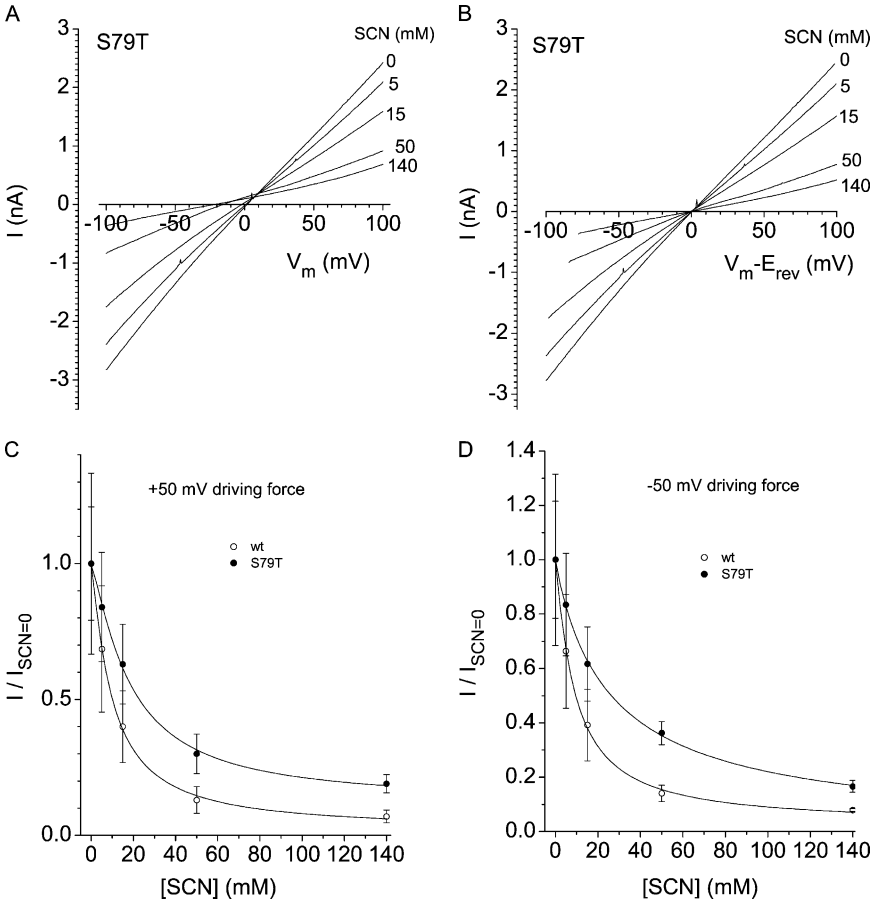

FIGURE 3. Block of mBest2-S79T–induced currents by extracellular SCN. (A) Current–voltage relationships in S79T-expressing cells with the external solutions in which Cl was replaced with equimolar amounts of [SCN] from 0 to 140 mM as indicated. (B) The I–V curves in A were replotted vs. the driving force (V_m–E_{rev}) for each SCN concentration. (C and D) Dose-dependent block by SCN at +50 mV (C) or −50 mV (D) driving force. The fractional currents at −50 mV (C) or +50 mV (D) driving force for each anion mixture were plotted as a function of [SCN] for wild type (open circles, $n = 4$) and the S79T mutant (filled circles, $n = 6$). The data points were fitted to the logistic equation. The wild-type data are from an experiment contemporaneous with the S79T experiment and agree with those we published previously (Qu et al., 2004).

These data raised the possibility that a similar time-dependent effect of SCN occurred in wild-type mBest2, but that it was not observed because it was fast relative to the 10-s interval between voltage clamp pulses that we used previously (Qu et al., 2004). However, when we used the more rapid protocol, we were still unable to see evidence for a time-dependent change in conductance with wild-type mBest2. There was no difference in the rate of change of E_{rev} and G_{slope} (Fig. 2 D). The apparent time constant for wild-type currents was 1.7 s, which is ~10-fold faster than for S79T (Fig. 2 C).

S79T Has Reduced Sensitivity to SCN

The above experiments suggested that SCN may bind more slowly to the S79T channel than to wild-type channels. To determine whether this was reflected in a decreased steady-state affinity of SCN for the S79T channel, we measured the ability of SCN to block Cl conductance in S79T-expressing cells. Different amounts of Cl were replaced with equimolar amounts of SCN, and the currents were measured in both wild-type and S79T channels. As we have previously reported (Qu et al., 2004), in wild-type mBest2, SCN blocked both inward and outward currents with the same IC_{50} (9.8 ± 1.1 mM, $n = 4$; Fig. 3, C and D). In S79T channels, the IC_{50}s were twofold larger: 18.5 ± 2.7 mM ($n = 6$) for outward current and 26.6 ± 6.0 mM for inward current (Fig. 3). This apparent lower affinity of the S79T channel is consistent with the slower reduction in channel conductance by SCN in the S79T mutant.

Effects of Mutations in Other Residues in the Region of S79

The data presented above and in our previous paper (Qu et al., 2004) suggested that S79 was part of an anion binding site in the mBest2 channel. We then explored the involvement of adjacent residues. Fig. 4 shows an alignment of residues 75–95 of the vertebrate bestrophins. It has been suggested that this domain comprises the second TMD (Tsunenari et al., 2003). Nathans' lab has shown that mutation of the residues shown in bold italics in hBest1 (residues 75, 76, 77, 81, 82, 85, 88, 89, 91, 92, 93, 95, and 96) to cysteine produces no current (Tsunenari et al., 2003). We focused, therefore, on V78, F80, G83, F84, V86, and T87.

The relative SCN and Cl conductances and permeabilities of these residues mutated to cysteine are shown in Fig. 5 (compare to wild type; Fig. 1, C and D). These mutations exhibited G_{SCN}/G_{Cl} ratios approximately six to nine times greater and P_{SCN}/P_{Cl} ratios 15–40% as large as wild type. This result resembles that found in ClC and

```
hBest1      75  LIPISFVLGFYVTLVVTRWWNQ  96
fBest1          LIPVSFVLGFYVTLVVSRWWGQ
ZfBest1         LIPVSFVLGFYVTLVVSRWWGQ
mBest1          LIPISFVLGFYVTLVVSRWWSQ
ratBest1        LIPISFVLGFYVTLVVTRWWNQ
fBest2          LIPMSFVLGFYVTLVVNRWWSQ
ZfBest2         LIPMSFVLGFYVTLVVNRWWSQ
XBest2          LIPVSFVLGFYVTLVVNRWWNQ
hBest2          LIPVSFVLGFYVTLVVNRWWSQ
mBest2          LIPVSFVLGFYVTLVVHRWWNQ
ratBest2        LIPVSFVLGFYVTLVVHRWWNQ
hBest3          QIPVTFVLGFYVTLVVNRWWNQ
mBest3          QIPVTFVLGFYVTLVVNRWWNQ
ratBest3        QIPVTFVLGFYVTLVVNRWWNQ
hBest4          LIPLSFVLGFYVTLVVNRWWSQ
mBest4          LIPLSFVLGFYVTLVVNRWWSQ
ratBest4        LIPLSFVLGFYVTLVVNRWWSQ
```

FIGURE 4. Alignment of TMD2 of vertebrate bestrophins. The putative second TMDs for human (h), Fugu (f), zebrafish (Zf), mouse (m), rat (rat), and *Xenopus* (X) bestrophins were aligned using the Clustal W algorithm. Identical amino acids are shaded. Amino acids in bold italics in hBest1 were shown not to produce currents when mutated to Cys (Sun et al., 2002; Tsunenari et al., 2003).

CFTR Cl channels (see DISCUSSION), where mutations throughout transmembrane segments alter anion selectivity in similar ways.

F80C Mutation Responds to MTS Modification Differently than S79C

Although the F80C mutation resembled the S79C mutation in some respects, the effects of MTS modification differed significantly. In S79C, both the negatively charged $MTSES^-$ and the positively charged $MTSET^+$ reagents stimulated the current. In contrast, with F80C, $MTSES^-$ reduced the current whereas $MTSET^+$ dramatically stimulated the current (Fig. 6). Both effects were reversed by DTT, although the effect of $MTSES^-$ was reversed more slowly than the effect of $MTSET^+$. Furthermore, the MTS reagents affected current rectification differently. $MTSET^+$ made the current outwardly rectify, whereas $MTSES^-$ made the current inwardly rectify more than control (Fig. 6, B and E). NEM, a neutral sulfhydryl reagent, had no effect on outward current, but inhibited inward current slightly and linearized the I–V relationship (Fig. 7, C and D). These data suggest that charge at position 80 could affect anion conductance of the channel: negative charge ($MTSES^-$) reduced while positive charge ($MTSET^+$) enhanced anion conduction. This suggests that position 80 is in electrostatic proximity to the conducting anion.

The relatively small effect of NEM could be explained if NEM reacted poorly with the cysteine at this position. To test this, we examined the effect of $MTSET^+$ after NEM treatment (Fig. 6 C). In this experiment, NEM produced little effect on outward current, but decreased inward current ~45%. After washing out NEM, $MTSET^+$ was added to the bath. This caused an increase in both inward and outward current, but the effect was significantly less than we found for cells that had not been exposed to NEM (Fig. 6 E). This suggests that a significant fraction of F80C residues had reacted with NEM so that these were now not available for reaction with $MTSET^+$.

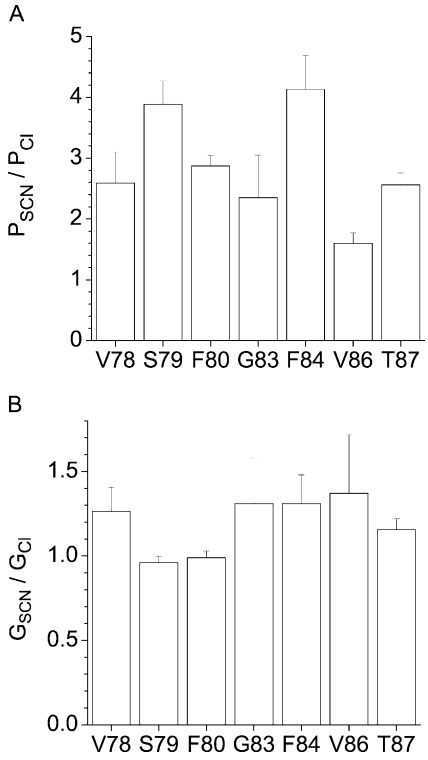

FIGURE 5. Mutations of V78C, F80C, G83C, F84, V86C, T87C in mBest2 change conductance and permeability to SCN. Experimental protocols are indicated in Fig. 1. (A) Relative permeabilities. (B) Relative conductance. Wild type ($n = 10$), F80C ($n = 6$), V78C ($n = 5$), G83C ($n = 3$), F84C ($n = 14$), V86C ($n = 4$), T87C ($n = 6$). Conductances and permeabilities were measured immediately after changing the solution to SCN.

Mutation of F80 to Arg or Glu

As a further test of the electrostatic effects at position 80, we mutated F80 into Arg or Glu. When F80 was mutated into Glu, the currents were either inwardly rectifying or very small (Fig. 7 A). These results are consistent with the effect of $MTSES^-$ modification, which also made the current inwardly rectifying and reduced the conductance (Fig. 6). In contrast, when F80 was mutated into positively charged Arg, the currents outwardly rectified (Fig. 7 B). These results are consistent with the effects of $MTSET^+$. Fig. 7 C plots the average rectification ratio (ratio of inward current at +50 mV to current at −50 mV) as a function of the charge located at position 80 in mBest2.

F80R Exhibits Voltage-dependent Block by DIDS

Currents in F80R-expressing cells were blocked by DIDS in a voltage-dependent manner (Fig. 8). With the F80R

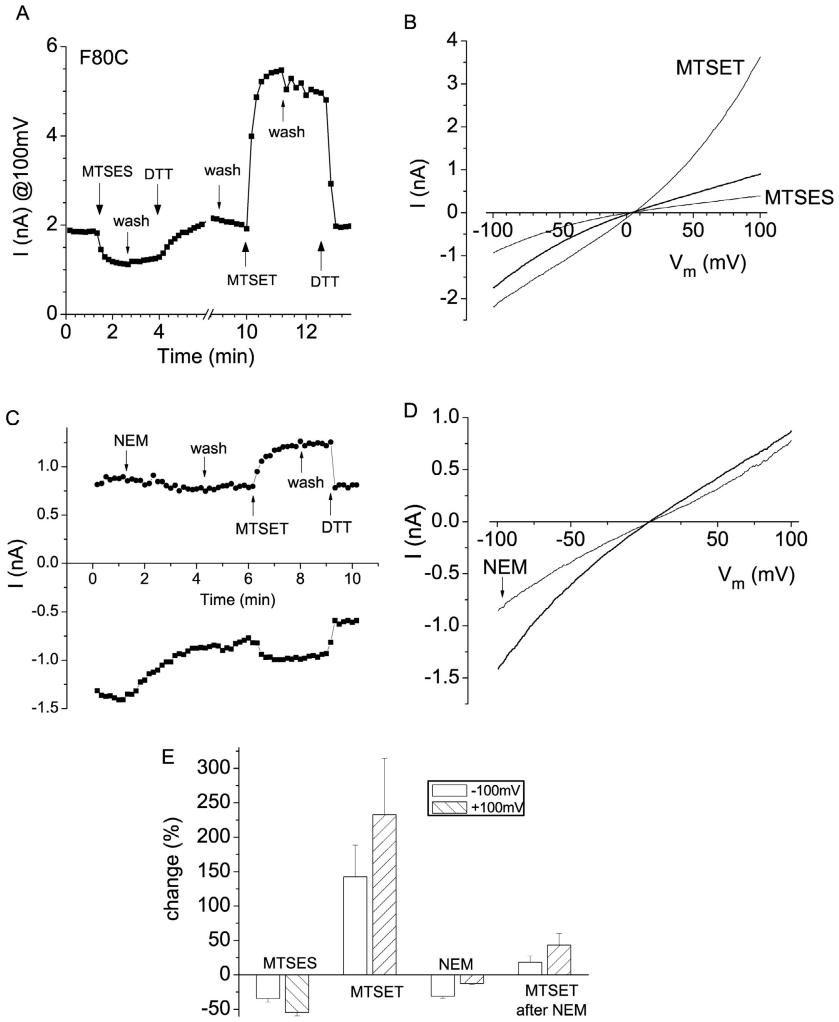

FIGURE 6. Effects of sulfhydryl modification on F80C currents. Cells were voltage clamped with a voltage ramp. (A) Time course of MTS reagent effects. The currents at +100 mV were plotted versus time. $MTSES^-$ (1 mM) or $MTSET^+$ (0.1 mM) was applied in bath solution. After washing, 5 mM DTT was used to reverse the effect of MTS modification. (B) Representative I–V curves for F80C mutant before (unlabeled curve) and after cell was exposed to $MTSES^-$ or $MTSET^+$. (C) Time course of effect of NEM and subsequent exposure to $MTSET^+$. (D) I–V curves for F80C mutant before (unlabeled curve) and after cell was exposed to NEM. (E) Summary of effects of sulfhydryl modification on F80C mutation. The percent change in currents at −100 mV (open bars) or +100 mV (hatched bars) produced by MTS modification. $MTSES^-$ ($n = 11$), $MTSET^+$ ($n = 8$), and NEM ($n = 5$).

mutant, 100 μM DIDS blocked the current ~90% at +100 mV, but only ~45% at −100 mV. In contrast, with wild type and the F80E mutant the block was voltage independent (Fig. 8 A). The F80E mutant was somewhat less sensitive to DIDS than wild type (Fig. 8 A). To analyze the voltage dependence of block of F80R, we measured the effect of different DIDS concentrations at different potentials between −100 mV and +100 mV and analyzed the data according to Woodhull (1973). The currents were more sensitive to DIDS at more positive potentials (Fig. 8 C). The apparent K_i decreased from 38.6 μM at 10 mV to 16 μM at 100 mV (Fig. 8, D and E). According to the Woodhull equation, this predicts that the binding site for DIDS is ~15% into the voltage field

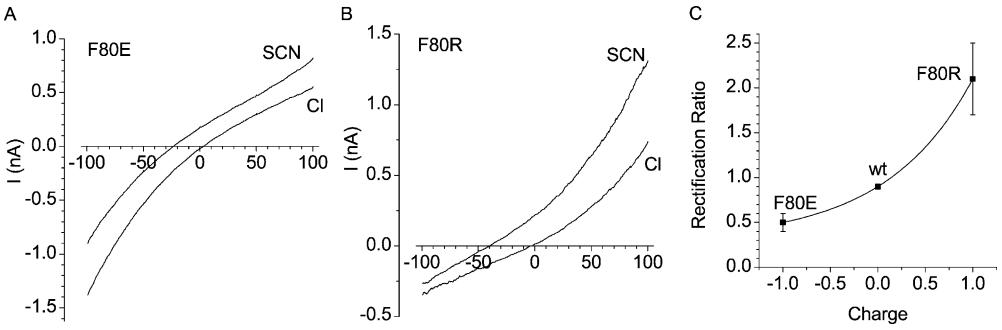

FIGURE 7. Mutations at position 80 change rectification ratios (RR) of mBest2 currents. (A) I–V curves reflecting inward rectification of F80E mutation in Cl or SCN. (B) F80R mutation makes currents outwardly rectifying in Cl or SCN. (C) Rectification ratio of mBest2-wild type (wt, $n = 17$), F80E ($n = 12$), and F80R ($n = 16$). The measurement for RR is described in MATERIALS AND METHODS.

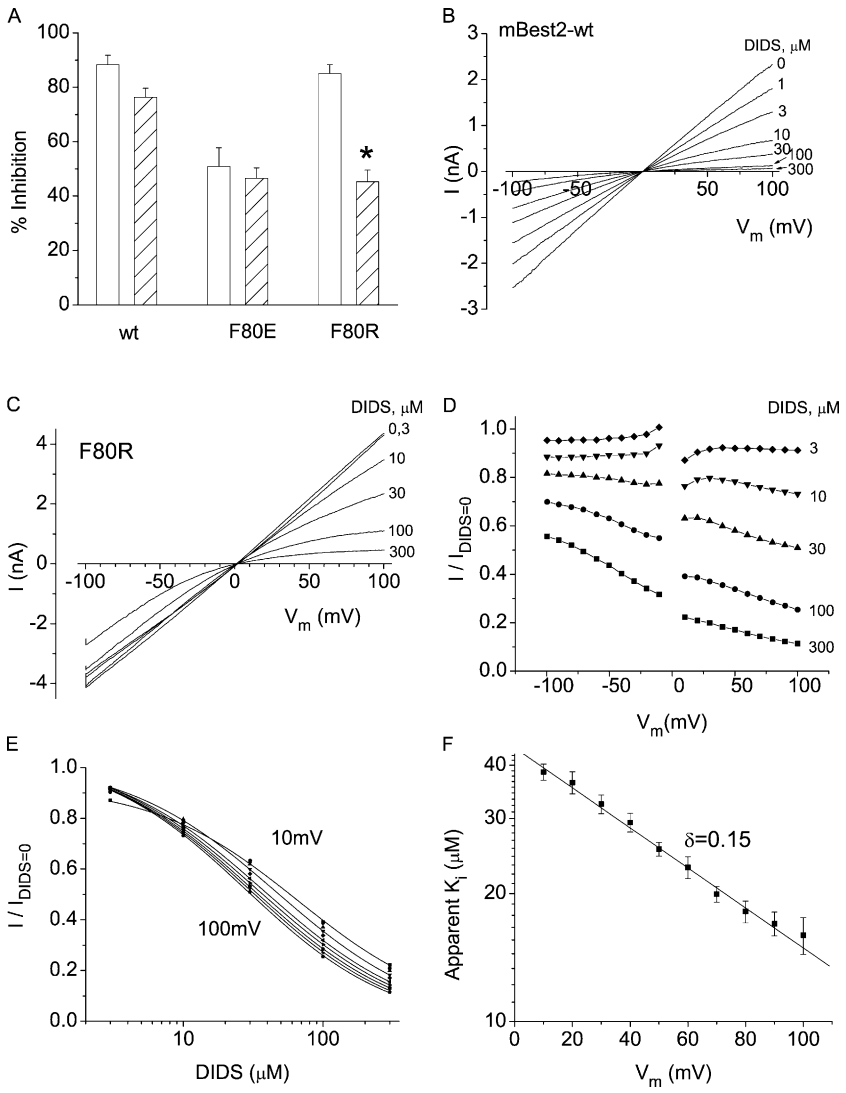

FIGURE 8. Voltage-dependent block of F80R currents by extracellular DIDS. (A) Effect of DIDS on currents induced in HEK cells expressing wild type ($n = 8$), F80E mutant ($n = 7$), and F80R mutant ($n = 7$) mBest2. DIDS (100 μM) was applied to the bath and percent inhibition of currents at +100 mV (open bars) and −100 mV (hatched bars) was measured. (B) Block of wild-type current by DIDS is not voltage dependent. The I–V curves show the voltage-independent block by various [DIDS] in bath solution as indicated. (C) I–V curves showing voltage-dependent block by DIDS of F80R currents. (D) Analysis of voltage-dependent block of F80R currents. Each curve from +10 to +100 mV in C was divided by the curve obtained in 0 μM DIDS. The fractional currents were plotted versus membrane potential. (E) [DIDS]-dependent block of F80R currents. The fractional currents at various potentials in D were replotted as function of [DIDS]. The data were fitted to logistic equation. (F) Voltage dependence of K_i of DIDS block. Apparent K_i at each voltage was determined from the fits in E in three separate experiments and averaged. The averaged K_i was plotted as a function of membrane potential. The points were fitted to Woodhull equation (Woodhull, 1973) (see text for further details).

of the membrane. The voltage dependence of DIDS block provides additional evidence that F80 is in the conduction pathway of the channel.

V78C Mutation Responds Differently than F80C or S79C to MTS Modification

Like S79C and F80C, the V78C mutation exhibited a P_{SCN}/P_{Cl} ratio that was less than wild type and a G_{SCN}/G_{Cl} ratio greater than wild type (Fig. 5). Interestingly, the effects of $MTSET^+$ and $MTSES^-$ were the opposite of those observed for F80C (Fig. 9). $MTSET^+$ reduced the current on average ~60%, whereas $MTSES^-$ stimulated the current approximately eightfold. The fact that F80C and V78C mutants respond oppositely to MTS reagents suggests that these residues have different proximities or relationships to the permeant anion. Because negative charge at position 80 inhibits current, this suggests that this position is closer to the narrowest region of the conduction pathway.

Effect of Mutations at S79 and F80 on Conduction of Other Anions

The data above provide reasonable evidence that S79 and F80 are located in the permeation pathway of the mBest2 channel and that these residues may contribute to anion binding by the channel. However, much of the evidence we have shown comes from experiments that compare permeability and conductance of SCN and Cl. If residues in TMD2 contribute to an anion binding site in the conduction pathway of the channel, we might expect that mutations in these residues would affect the permeation and conductance of other anions in addition to SCN. Table I shows the relative permeability and conductance for Br, I, NO_3, and SCN for the wild-type mBest2 and for the F80C, S79C, and F80R mutations. For the wild-type channel, the relative permeabilities were $SCN > NO_3 = I > Br > Cl$. The relative conductances were $NO_3 > I > Cl \geq Br > SCN$. None of the three mutations altered the permeability or conduc-

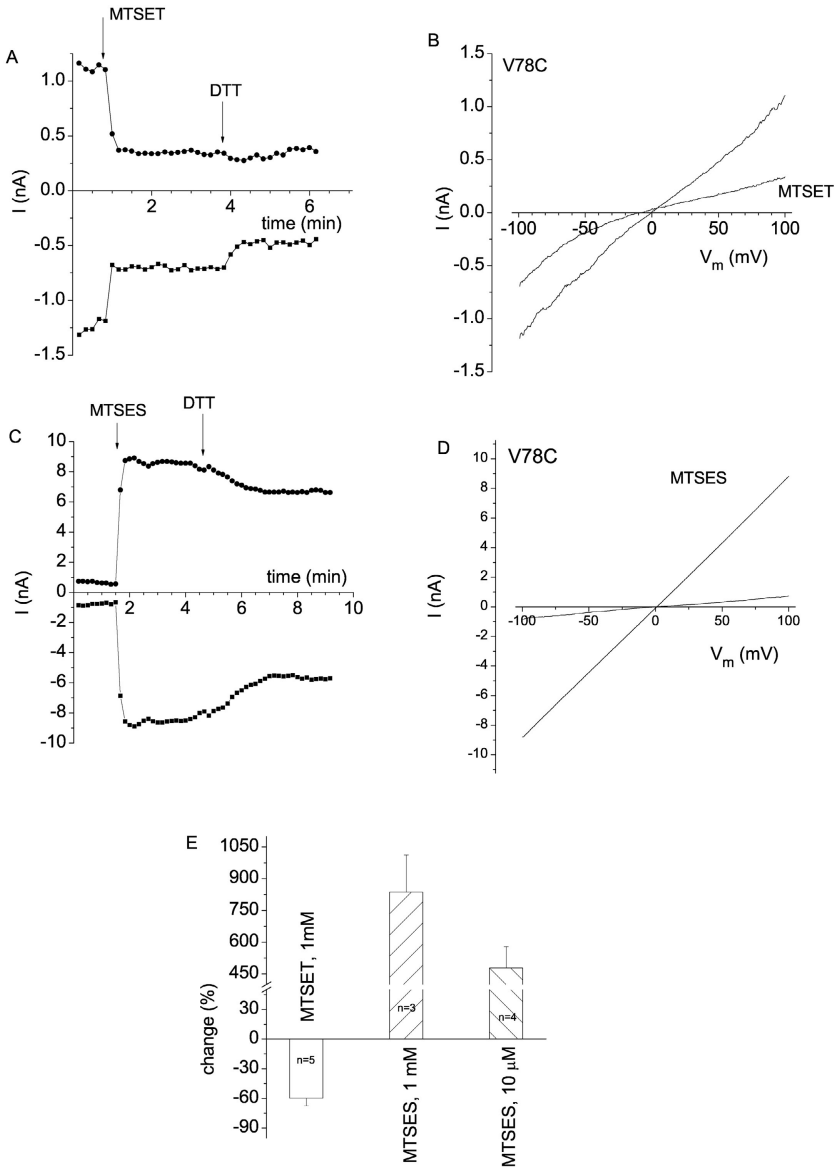

FIGURE 9. Effects of sulfhydryl reagents on V78C currents. Experiments were performed as in Fig. 7. (A) Time course of effect of $MTSET^+$ and reversibility by DTT. 1 mM MTSET or 5 mM DTT were applied at times indicated. Currents were measured at +100 mV (upper panel) and −100 mV (lower panel). (B) I–V curves showing inward rectification of currents produced by $MTSET^+$. (C) Time course of effect of $MTSES^-$. 1 mM $MTSES^-$ or 5 mM DTT was applied as indicated. (D) I–V curve of currents stimulated by $MTSES^-$ application. (E) Average effect of MTS reagents on V78C currents. *n* is shown within the bars.

tance sequence significantly. The only possible exception to this generalization was in the F80R mutation, where $G_I > G_{Br}$ was changed to $G_I = G_{Br}$. In all three mutations, P_{SCN}/P_{Cl} was reduced, G_{SCN}/G_{Cl} was enhanced, and G_{NO3}/G_{Cl} was decreased.

DISCUSSION

Mutations in TMD2 Alter Anion Permeation and Conduction

In this paper, we have explored in detail the contribution of serine-79 and other residues in TMD2 to determining the conductance and permeability of mBest2. Replacement of the natural amino acid with cysteine had very similar effects at positions 78, 79, 80, 83, 84, 86, and 87: the relative permeability of the channel to SCN was decreased relative to Cl and the relative conductance of the current was increased. The effects of charged sulfhydryl-reactive MTS reagents differed qualitatively at position 78, 79, and 80. In the V78C mutant, positively charged MTSET inhibited while the negatively charged MTSES stimulated the current. In F80C, the effects were the opposite to those in V78C: MTSET stimulated and MTSES inhibited the current. In the S79C, both MTSET and MTSES were stimulatory. S79 and F80 also behave differently when the native amino acid is replaced with charged amino acids. Replacement of serine-79 with either Arg or Glu had the same effect as replacement with Cys: P_{SCN}/P_{Cl} was decreased and G_{SCN}/G_{Cl} was increased. In contrast, with F80, substitution with Arg resulted in outward rectification, whereas substitution with Glu resulted in inward rectification. The different effects of charged MTS reagents and of substitution of charged amino acids suggest that although each of these residues is involved in anion

permeation, their contributions are somewhat different. Because ion permeability and conduction are controlled by the partitioning of the ion into the channel pore and the binding of the ion to sites in the permeation pathway, the data above provide prima facie evidence that bestrophins form the pore of the Cl channel.

Mutations in Cl Channel Pores Generally Have Relatively Modest Effects on Selectivity

In identifying the amino acid residues that define the pore of the bestrophins, one would like to find a point mutation that dramatically alters the selectivity of the channel. The most dramatic example would be conversion of the channel from anion selective to cation selective. Such a change in selectivity has been reported for the A251E mutation in glycine receptors (Keramidas et al., 2002a). Such a dramatic switch in selectivity is possible to engineer in glycine receptors probably because their selectivity is largely due to electrostatic interactions of the permeant anion with basic residues in the channel pore. The converse substitutions convert the nAChR from cation selective to anion selective (Galzi et al., 1992). It has not been possible to convert voltage-gated and inwardly rectifying K channels into anion channels, but discrete mutations in any one of four residues in the K channel signature sequence have quantitatively dramatic effects on K selectivity. For example, mutation of either of the glycine residues in the TMT-TVGYG sequence in the Shaker channel abolishes K selectivity (Heginbotham et al., 1994). K channels normally select K:Na by ~100:1, but in the G to A mutant, Na and K have about equal permeabilities. Mutations in the signature sequence can be grouped into two groups, ones that have little effect on selectivity and ones that abolish selectivity among cations altogether. The mutations that abolish selectivity probably do so because they produce major structural changes in pore structure.

In contrast, mutational analysis of amino acids in Cl channel pores (with the exception of ligand-gated anion channels) does not produce such discrete outcomes, probably because these channels are not as highly selective as voltage-gated cation channels. In the ClC family, for example, four stretches of amino acids that are not contiguous in the primary sequence contribute to forming the selectivity filter (Jentsch et al., 2002). Mutation of almost every amino acid in these domains changes anion selectivity (Fahlke, 2001). In human ClC-1, for example, mutation of 17/19 amino acid residues in these regions alters channel selectivity (Fahlke et al., 1997). Moreover, the effects of these mutations are relatively modest. For example, one of the mutations (G233A) in the human ClC-1 channel that produces the largest changes in relative permeability increases P_{SCN}/P_{Cl} only approximately eightfold and increases P_{NO3}/P_{Cl} and P_I/P_{Cl} only approximately threefold, compared with the 100-fold changes in Na/K selectivity produced by mutations in Shaker.

A similar situation exists with CFTR (Dawson et al., 1999). The pore of CFTR is comprised of residues in both TMD6 and TMD11. Indeed, although numerous mutations within the transmembrane regions of CFTR alter anion binding and single channel conductance, most mutations have rather little effect on anion selectivity. Even mutations that alter the selectivity sequence, such as F337A, do so by less than fourfold changes in relative permeabilities (Linsdell et al., 2000). These data have led Dawson and colleagues to propose that the detailed structure of the CFTR pore may not be a major factor determining anion selectivity (Dawson et al., 1999; Smith et al., 1999, 2001). Rather, they propose that permeation is determined largely by the ease with which an anion partitions into the channel, which is a function of how easily the anion exchanges its water of hydration with residues in the channel. As long as the pore provides an adequately hydrophilic environment for the permeating anion, small perturbations in channel structure may not alter the permeability.

Perturbation of Selectivity in mBest2 by Mutations in TMD2

Our results with mBest-2 are comparable to those reported for ClCs and CFTR with regard to the relatively modest changes that mutations confer on channel selectivity. We find that the largest effects of mutations in S79 and F80 on permeability were evident only with SCN as the permeant anion. P_{SCN}/P_{Cl} was changed greater than fivefold, but NO_3, I, and Br permeabilities were not significantly affected. This is similar to the effect of pore mutations in hClC-1 and CFTR that affected relative SCN permeability more than the relative permeability of smaller anions. Furthermore, in mBest2, there was not a single amino acid residue that exhibited priority in determining anion permeability: mutations in V78, S79, F80, G83, F84, V86, and T87 altered selectivity in similar manners. This suggests that, like CFTR and the ClCs, certain details of the structure of the pore may not be crucial in determining anion permeation. Permeation may simply depend on ions partitioning into a hydrophilic channel, and as long as the channel maintains this hydrophilic pore, permeation occurs relatively normally. It should be emphasized that cysteine mutations at 10 positions in TMD2 (75, 76, 77, 81, 82, 85, 88, 89, 91, and 92) result in nonfunctional channels. These mutations may result in disruption of the channel pore structure sufficiently so that the channel is not capable of acting as an aqueous pore for anions.

The suggestion that the specific structure of the channel pore is relatively unimportant in selectivity is

supported by our observation that qualitatively similar effects on channel permeability are produced by substitutions at positions 79 and 80 with amino acids having a diversity of side chains. For example, P_{SCN}/P_{Cl} and G_{SCN}/G_{Cl} were similar in the S79A, S79E, and S79R mutants. The ability of mBest2 to continue to function as a Cl channel, albeit with different selectivity than the wild type, in the light of presumed major changes in the putative pore domain suggest that either TMD2 is not actually the pore domain or that the mechanisms of selectivity do not rely on the amino acid side chains, at least when they are altered one at a time.

The role of electrostatic interactions in the mBest2 pore remains unclear. Within the putative TMD2, the only positively charged residue is R92. Nathans and coworkers have reported that the R92C mutation in hBest1 produced no current (Tsunenari et al., 2003). The fact that introduction of charge at position F80 produces changes in rectification suggest that F80 is in close proximity to the permeant anion, but the absence of a charged residue in the native protein in TMD2 suggests that either the electrostatic environment of the pore may not be important in permeation or that charged residues are contributed from other regions of the mBest2 protein that we have not yet investigated in detail.

Channel Gating

Because we have measured macroscopic currents, we do not know whether the changes in relative conductance that occur as a consequence of mutations are caused by changes in single channel conductance or channel gating. However, the observation that the time course of change in conductance in the S79T mutant lags significantly behind the change in E_{rev} provides support to the idea that the decreased conductance produced by SCN is due at least partially to changes in channel gating. One would predict that, if the small G_{SCN}/G_{Cl} in wild-type mBest2 was a consequence of a smaller flux of SCN relative to Cl though the channel, the effect of SCN would occur instantaneously. That is, if G_{SCN}/G_{Cl} is due entirely to the binding of SCN to a site in the selectivity filter of the channel, this should occur as soon as SCN begins to permeate the channel, as evidenced by the shift in the E_{rev}. However, the fact that this change takes about a minute to reach completion in the S79T mutant suggests that it takes some time for SCN to reach its binding site. If this is the case, the binding site may not be in the permeation pathway and that G_{SCN}/G_{Cl} may be determined by binding of SCN to an allosteric site in the channel, possibly on the cytoplasmic side. The observation that block of current by SCN is not detectably voltage dependent supports the suggestion that the SCN binding site is not in the selectivity filter. However, the observation that DIDS blocks the current induced by the F80R mutant in a voltage-dependent manner argues that F80 is located in the voltage field of the membrane.

Topology of mBest2

Tsunenari et al. (2003) have proposed a topology model for hBest1 based on insertion of N-linked glycosylation sites and TEVP protease cleavage sites as well as the effects of membrane-impermeant sulfhydryl reagents on hBest1 currents. From these data, they propose that hBest1 has four TMDs and that TMD2 crosses the membrane from outside to inside in the NH_2- to COOH-terminal direction. However, some of their data is inconsistent with this interpretation. Their data show clearly that residues C69 and N99 are accessible to the extracellular space, whereas their model places these residues at the opposite ends of TMD2. Their evidence is based on modification of hBest1 currents by the membrane-impermeant sulfhydryl reagent $MTSET^+$. Modification of the native C69 residue with extracellular $MTSET^+$ inhibits hBest1 current, so C69 is extracellular. The C69A mutant is unaffected by $MTSET^+$, confirming that the effect of $MTSET^+$ is on C69. N99 is also thought to be extracellular because extracellular $MTSET^+$ inhibits the current produced by the C69A/N99C mutant. Intracellular cysteine does not quench the effect of $MTSET^+$ on the C69A/N99C mutant, showing that $MTSET^+$ does not permeate the channel. It seems impossible that both C69 and N99 are extracellular if this sequence is truly transmembrane.

There are differences between hBest1 and mBest2 that raise additional questions. First, although position 69 is Cys in both mBest2 and hBest1, $MTSET^+$ inhibits the hBest1 current via C69 (Tsunenari et al., 2003) but has no effect on wild-type mBest2 current (Qu et al., 2004). Second, although mutation of N99 to Cys in hBest1 results in a current that is sensitive to $MTSET^+$, the wild-type residue in mBest2 at position 99 is Cys, but wild-type mBest2 is not sensitive to MTSET. Is it possible that mBest2 and hBest1 have different topologies or do the mutations cause major structural rearrangements that are confounding the interpretations?

Our data with DIDS block of the F80R mutated channel suggest that this residue is 15% of the way into the voltage field from the outside of the cell. Furthermore, we find that residues from 78 to 87 are accessible to MTS reagents applied from the outside of the cell. These data suggest that this region of mBest2 is in an outer vestibule of the channel.

The authors thank Chun Pfahnl and Toni Grim for excellent technical assistance, Drs. Rodolphe Fischmeister and Ilva Putzier for helpful discussion, and Ms. Li-Ting Chien for help with experiments on F84C.

This work was supported by National Institutes of Health grants GM60448 and EY014852 to H.C. Hartzell and American

Heart Association Scientist Development Grant 0430204N to Z. Qu.

David C. Gadsby served as editor.

Submitted: 21 May 2004
Accepted: 18 August 2004

REFERENCES

Armstrong, C.M. 2003. Voltage-gated K channels. *Sci. STKE.* 2003: re10.

Dawson, D.C., S.S. Smith, and M.K. Mansoura. 1999. CFTR: mechanism of anion conduction. *Physiol. Rev.* 79:S47–S75.

Deutman, A.F. 1969. Electro-oculography in families with vitelliform dystrophy of the fovea. Detection of the carrier state. *Arch. Ophthalmol.* 81:305–316.

Dutzler, R., E.B. Campbell, M. Cadene, B.T. Chait, and R. MacKinnon. 2002. X-ray structure of a ClC chloride channel at 3.0 A reveals the molecular basis of anion selectivity. *Nature.* 415:287–294.

Fahlke, C. 2001. Ion permeation and selectivity in ClC-type chloride channels. *Am. J. Physiol. Renal. Physiol.* 280:F748–F757.

Fahlke, C., H.T. Yu, C.L. Beck, T.H. Rhodes, and A.L. George Jr. 1997. Pore-forming segments in voltage-gated chloride channels. *Nature.* 390:529–532.

Francois, J., A. De Rouck, and D. Fernandez-Sasso. 1967. Electro-oculography in vitelliform degeneration of the macula. *Arch. Ophthalmol.* 77:726–733.

Gallemore, R.P., B.A. Hughes, and S.S. Miller. 1998. Light-induced responses of the retinal pigment epithelium. *In* The Retinal Pigment Epithelium. M.F. Marmor and T.J. Wolfensberger, editors. Oxford University Press, Oxford. 175–198.

Galzi, J.L., A. Devillers-Thiery, N. Hussy, S. Bertrand, J.P. Changeux, and D. Bertrand. 1992. Mutations in the channel domain of a neuronal nicotinic receptor convert ion selectivity from cationic to anionic. *Nature.* 359:500–505.

Hartzell, H.C., and Z. Qu. 2003. Chloride currents in acutely isolated *Xenopus* retinal pigment epithelial cells. *J. Physiol.* 549:453–469.

Heginbotham, L., Z. Lu, T. Abramson, and R. MacKinnon. 1994. Mutations in the K^+ channel signature sequence. *Biophys. J.* 66: 1061–1067.

Jentsch, T.J., V. Stein, F. Weinreich, and A.A. Zdebik. 2002. Molecular structure and physiological function of chloride channels. *Physiol. Rev.* 82:503–568.

Keramidas, A., A.J. Moorhouse, C.R. French, P.R. Schofield, and P.H. Barry. 2002a. M2 pore mutations convert the glycine receptor channel from being anion- to cation-selective. *Biophys. J.* 79: 247–259.

Keramidas, A., A.J. Moorhouse, K.D. Pierce, P.R. Schofield, and P.H. Barry. 2002b. Cation-selective mutations in the M2 domain of the inhibitory glycine receptor channel reveal determinants of ion-charge selectivity. *J. Gen. Physiol.* 119:393–410.

Kuruma, A., and H.C. Hartzell. 2000. Bimodal control of a Ca^{2+}-activated Cl^- channel by different Ca^{2+} signals. *J. Gen. Physiol.* 115:59–80.

Linsdell, P., A. Evagelidis, and J.W. Hanrahan. 2000. Molecular determinants of anion selectivity in the cystic fibrosis transmembrane conductance regulatory chloride channel pore. *Biophys. J.* 78:2973–2982.

Marmorstein, A.D., L.Y. Mormorstein, M. Rayborn, X. Wang, J.G. Hollyfield, and K. Petrukhin. 2000. Bestrophin, the product of the Best vitelliform macular dystrophy gene (VMD2), localizes to the basolateral membrane of the retinal pigment epithelium. *Proc. Natl. Acad. Sci. USA.* 97:12758–12763.

Petrukhin, K., M.J. Koisti, B. Bakall, W. Li, G. Xie, T. Marknell, O. Sandgren, K. Forsman, G. Holmgren, S. Andreasson, et al. 1998. Identification of the gene responsible for Best macular dystrophy. *Nat. Genet.* 19:241–247.

Pusch, M. 2004. Ca^{2+}-activated chloride channels go molecular. *J. Gen. Physiol.* 123:323–325.

Qu, Z., R. Fischmeister, and H.C. Hartzell. 2004. Mouse bestrophin-2 is a bona fide Cl^- channel: identification of a residue important in anion binding and conduction. *J. Gen. Physiol.* 123: 327–340.

Qu, Z., and H.C. Hartzell. 2000. Anion permeation in Ca-activated Cl channels. *J. Gen. Physiol.* 116:825–844.

Qu, Z., and H.C. Hartzell. 2003. Two bestrophins cloned from *Xenopus laevis* oocytes express Ca-activated Cl currents. *J. Biol. Chem.* 278:49563–49572.

Smith, S.S., E.D. Steinle, M.E. Meyerhoff, and D.C. Dawson. 1999. Cystic fibrosis transmembrane conductance regulator: physical basis for lyotropic anion selectivity patterns. *J. Gen. Physiol.* 114: 799–817.

Smith, S.S., X. Liu, Z.R. Zhang, F. Sun, T.E. Kriewall, N.A. McCarty, and D.C. Dawson. 2001. CFTR: covalent and noncovalent modification suggests a role for fixed charges in anion conduction. *J. Gen. Physiol.* 118:407–432.

Sun, H., T. Tsunenari, K.-W. Yau, and J. Nathans. 2002. The vitelliform macular dystrophy protein defines a new family of chloride channels. *Proc. Natl. Acad. Sci. USA.* 99:4008–4013.

Tsien, R.Y., and T. Pozzan. 1989. Measurements of cytosolic free Ca^{2+} with Quin-2. *Methods Enzymol.* 172:230–262.

Tsunenari, T., H. Sun, J. Williams, H. Cahill, P. Smallwood, K.-W. Yau, and J. Nathans. 2003. Structure-function analysis of the bestrophin family of anion channels. *J. Biol. Chem.* 278:41114–41125.

Woodhull, A.M. 1973. Ionic blockage of sodium channels in nerve. *J. Gen. Physiol.* 61:687–708.